

Optimization of Brake Judder Based on Dynamic Model of Disc-Pads Spring Contact



Gongyu Pan, Yaqi Feng, Peng Liu, Qizhao Xu, and Lin Chen

Abstract In order to predict the brake judder more accurately, the mechanism of brake judder was studied. First, a dynamic model of braking system based on surface-to-surface contact between disc and pads was constructed. The correctness of the model was verified by comparing the results of bench test and simulation. Then, the key parameters of brake judder were found from the calculation expressions of brake pressure variation (BPV) and brake torque variation (BTV), and two optimization directions were proposed to improve the structure of brake caliper and brake pad backplate. Finally, a method to determine parameters of the improved disc brake was proposed, which combined the finite element analysis with theoretical calculation. The parameters of the improved disc brake were substituted into the Simulink model of the dynamic model, and the time-domain responses of BPV and BTV were obtained. The results show that the maximum BPV and the maximum BTV of the optimized braking system are reduced by 30.7% and 34.2%, respectively, thus testifying to the correctness of the optimization method of brake judder proposed in this paper. The research method proposed in this paper had a certain contribution to the study of brake judder of disc brake. It not only improved the quantization accuracy of brake judder, but also reduced the probability of brake judder greatly. Therefore, this study has a certain engineering significance.

Keywords Brake judder optimization · Surface spring contact · Parameter determination · Brake torque variation · Brake pressure variation

G. Pan · Y. Feng (✉) · P. Liu
Jiangsu University, Zhenjiang 212013, China
e-mail: fyq15751011272@163.com

G. Pan · Q. Xu · L. Chen
Jiangsu Hengli Brake Manufacturing Co., Ltd, Taizhou 214500, China

© The Author(s), under exclusive license to Springer Nature Singapore Pte Ltd. 2023
W. Wang et al. (eds.), *Green Transportation and Low Carbon Mobility Safety*,
Lecture Notes in Electrical Engineering 944,
https://doi.org/10.1007/978-981-19-5615-7_26

367

1 Introduction

When people pay more and more attention to drive comfort, brake judder has become an important problem affecting the comfort of drivers and passengers [1]. Brake judder is a kind of low-frequency vibration, which can be transmitted to the steering wheel, brake pedal, seat rail and body floor through the steering system, caliper system and brake hydraulic pipeline [2, 3]. The external vibration caused by it can greatly affect the driver's comfort, and at the same time, driving fatigue and misoperation caused by it have affected the driver's driving safety [4]. In addition, brake judder also causes great harm to the service life of the braking system, which increases the maintenance cost of vehicles. Therefore, it is of great significance to take measures to reduce the brake judder of automobiles.

At present, many scholars have tried to reduce brake judder by improving the structure of brake components. Sim et al. [5] obtained the structural design parameters of the brake disc sensitive to brake judder through the sensitivity analysis method, and proposed an optimization method for reducing brake judder. Bryant et al. [6] optimized the shape of the brake disc ventilation groove to reduce brake judder. According to the response surface analysis method, Jung et al. [7] optimized the design parameters of the ventilation disc to reduce the maximum temperature and thermal deformation of disc, thus reducing the occurrence of thermal judder.

However, there are few studies on brake judder from the perspective of the dynamic model of the brake system. Leslie [8] proposed a brake caliper dynamic model which could be used to predict the level of BTV at a given DTV input. In order to reduce the level of BTV, the sensitivity of brake torque variation to the stiffness of brake components was studied. Zhang et al. [9] established a single point contact brake dynamic model to predict brake pressure variation, brake torque variation and caliper vibration acceleration in Matlab/Simulink software, and verified the validity of the model by simulation and test. Most of the existing brake dynamic models are in the form of single-point contact or multi-point contact, which have low quantitative accuracy for brake judder and cannot be better helpful for brake judder analysis and control.

In this paper, a disc-pads surface contact dynamic model of disc brake which is more in line with the actual contact situation is proposed to improve the accuracy of predicting brake judder. On this basis, a method to reduce brake judder by simultaneously improving caliper and brake pads is presented. The optimization result is validated by performing the judder analysis of the original and optimized disc brake.

2 Disc-Pads Surface Contact Dynamic Model of Disc Brake

2.1 Premises of Model Construction

In this paper, the following assumptions are made when constructing the disc-pads surface contact model of disc brake.

- (1) The braking system can be simplified as a multi-degree-of-freedom particle-spring system.
- (2) In this model, the surface distributed spring contact mode is used between disc and pad, and other parts are point-to-point contact mode.
- (3) The effect of brake pressure variation on friction characteristics between brake friction pairs is ignored, but the influence of the relative velocity between brake disc and brake block on the friction characteristics is considered.
- (4) The influence of thermal factor is not considered.

Based on the above assumptions, this paper takes the initial disc thickness variation (DTV) and surface run-out (SRO) of brake disc with brake judder phenomenon as input, BPV and BTV as output for simulation analysis to study the mechanism of brake judder and put forward the optimization scheme for brake judder.

2.2 Dynamic Model of Brake

The disc-pads surface contact dynamic model of disc brake proposed in this paper is shown in Fig. 1. The basic method taken in model development was to divide the braking system into constitutive mass/stiffness elements [8]. This model includes brake disc, outer brake block, inner brake block, calipers, piston and caliper bracket, which is immovable. The components were connected by springs and dampers. In this model, the single-point contact mode in the existing model was adopted between inner brake block and piston, between piston and caliper, and between outer brake block and caliper, while the surface-to-surface contact mode proposed in this paper was adopted between brake disc and brake block. This simplified brake dynamic model for analysis of brake judder mechanism has been recognized in recent years [8–11].

When braking, the brake pedal force is transmitted to the brake wheel cylinder through the hydraulic system, and the piston under hydraulic pressure presses the inner brake pad against the brake disc surface. Due to the surface run-out on one side of the brake disc, the brake pad is forced to vibrate in the direction perpendicular to the surface of the brake disc. When the brake pad is pressed against the surface of the brake disc, the inner brake pad is subjected to friction along the rotating direction of the brake disc due to the rotation of the brake disc, so that friction is generated between brake pad and piston surface. In the tangential direction, the movement of the brake pad is limited by the caliper holder. The outer brake pad is in direct contact

$$\begin{aligned}
 & + r^2 (\ddot{w}_{dr}(r))^2]dr \times \int_0^{2\pi} (w_{d\varphi}(\varphi))^2 d\varphi + 2(1 - \nu) \\
 & \times \int_{r_1}^{r_2} \frac{1}{r^3} (w_{dr}(r) - r \dot{w}_{dr}(r))^2 dr \times \int_0^{2\pi} (\dot{w}_{d\varphi}(\varphi))^2 d\varphi \\
 & + \int_{r_1}^{r_2} \frac{1}{r^3} (w_{dr}(r))^2 dr \int_0^{2\pi} (\ddot{w}_{d\varphi}(\varphi))^2 d\varphi \\
 & + \int_{r_1}^{r_2} \frac{2}{r^2} w_{dr}(r) (\dot{w}_{dr}(r) + \nu r \ddot{w}_{dr}(r)) dr \\
 & \times \int_0^{2\pi} w_{d\varphi}(\varphi) \ddot{w}_{d\varphi}(\varphi) d\varphi \left. \vphantom{\int_0^{2\pi}} \right\} (q_d(t))^2 \tag{2}
 \end{aligned}$$

In the above, D is the bending stiffness of the brake disc; ν is Poisson’s ratio.

The kinetic energy and potential energy of inner brake block are expressed by Eqs. (3) and (4), respectively.

$$T_{p1} = \frac{1}{2} m_{p1} \dot{w}_{p1}^2 + \frac{1}{2} (m_{p1} L_{11}^2 + I_{p1}) \dot{\theta}_i^2 \tag{3}$$

where m_{p1} is the mass of inner brake block; I_{p1} is the inertia moment; w_{p1} is the axial displacement of inner brake block; θ_i is the rotation angle of inner brake block around point P_{11} ; L_{11} is the distance between the center of mass of inner brake block and the connecting point of brake block and caliper bracket.

$$\begin{aligned}
 V_{p1} & = \frac{1}{2} (K_{ap} + K_h) w_{p1}^2 - K_h L_{11} w_{p1} \theta_i \\
 & + \frac{1}{2} (K_{11} + K_h L_{11}^2) \theta_i^2 \tag{4}
 \end{aligned}$$

In Eq. (4), K_{ap} is stiffness of abutment shim between pad and bracket; K_h is the interface stiffness between inner brake block and piston; K_{11} is the rotational stiffness of inner brake block around point P_{11} .

Similarly, the kinetic energy and potential energy of outer brake block are expressed by Eqs. (5) and (6), respectively.

$$T_{p2} = \frac{1}{2} m_{p2} \dot{w}_{p2}^2 + \frac{1}{2} (m_{p2} L_{12}^2 + I_{p2}) \dot{\theta}_o^2 \tag{5}$$

where m_{p2} is the mass of outer brake block; I_{p2} is the inertia moment; w_{p2} is the axial displacement of outer brake block; θ_o is the rotation angle of outer brake block

around point P_{12} ; L_{12} is the distance between the center of mass of outer brake block and the connecting point of brake block and caliper bracket.

$$V_{p2} = \frac{1}{2}(K_{ap} + K_{pc})w_{p2}^2 - (K_{pc}L_{12})w_{p2}\theta_o + \frac{1}{2}(K_{12} + K_{pc}L_{12}^2)\theta_o^2 \tag{6}$$

where K_{12} is rotational stiffness of outer brake block around point P_{12} ; K_{pc} is contact stiffness between outer brake block and caliper.

The kinetic and potential energy of piston can be expressed as follows.

$$T_h = \frac{1}{2}m_h\dot{w}_h^2 \tag{7}$$

In the above, m_h is the mass of piston; w_h is the axial displacement of piston.

$$V_h = \frac{1}{2}K_{hc}w_h^2 \tag{8}$$

where K_{hc} is equivalent hydraulic stiffness of wheel cylinder.

The Lagrangian function is:

$$L = T_d + T_{p1} + T_{p2} + T_h - V_d - V_{p1} - V_{p2} - V_h \tag{9}$$

By substituting each value into the above equation, the following equation of motion can be obtained.

$$M\ddot{w} + C\dot{w} + Kw = 0 \tag{10}$$

In the above, M , C and K are the mass, stiffness and damping matrices, respectively; w is the displacement matrix.

According to Fig. 1, brake pressure (P_B) and brake torque (T_B) can be expressed by Eqs. (11) and (12), respectively.

$$P_B = P_0S + (w_h - w_c)K_{hc} + (\dot{w}_h - \dot{w}_c)C_{hc} \tag{11}$$

where P_0 is initial braking pressure; S is the contact area of piston; w_c is the axial displacement of caliper; C_{hc} is equivalent hydraulic damping of wheel cylinder.

$$T_B = \mu_p \cdot R_{eff} \cdot [2P_0S + (w_{ri} - w_{p1})K_p + (\dot{w}_{ri} - \dot{w}_{p1})C_p + (w_{p2} - w_{ro})K_p + (\dot{w}_{p2} - \dot{w}_{ro})C_p] \tag{12}$$

where μ_p is the coefficient of friction between pads and disc; R_{eff} is the brake effective radius; w_{ri} and w_{ro} are the displacements of inner and outer surface of disc, respectively; K_p and C_p are the dynamic compressive stiffness and damping of brake block, respectively.

Thus, BTV and BPV can be respectively expressed as:

$$P_{BPV} = (w_h - w_c)K_{hc} + (\dot{w}_h - \dot{w}_c)C_{hc} \tag{13}$$

$$T_{BTV} = \mu_p \cdot R_{eff} \cdot [(w_{ri} - w_{p1})K_p + (\dot{w}_{ri} - \dot{w}_{p1})C_p + (w_{p2} - w_{ro})K_p + (\dot{w}_{p2} - \dot{w}_{ro})C_p] \tag{14}$$

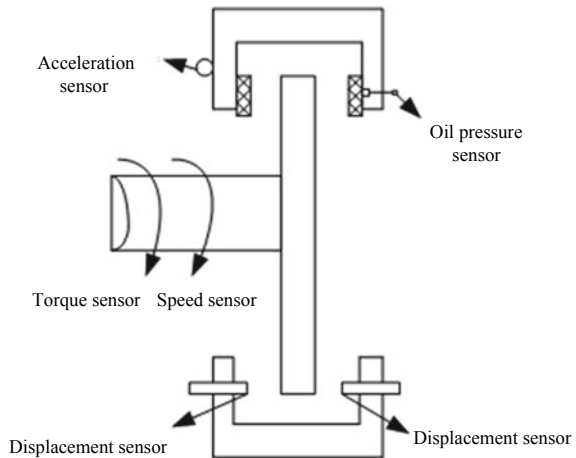
The values of all parameters involved in Fig. 1 and Eqs. (1)–(14) are listed in Appendix A.

2.3 Input of Model

Brake dynamo test was done using LINK model 3900. The disc brake with brake judder problem was employed in the test. The arrangement of measuring points in this test is shown in Fig. 2.

The brake disc thickness variation and surface runout measured by displacement sensors are superimposed as the system input. The initial DTV of the brake disc can be obtained by taking the thickness variation of disc during the uniform rotation of rotor at the initial braking speed, as shown in Fig. 3.

Fig. 2 Layout diagram bench test measuring points



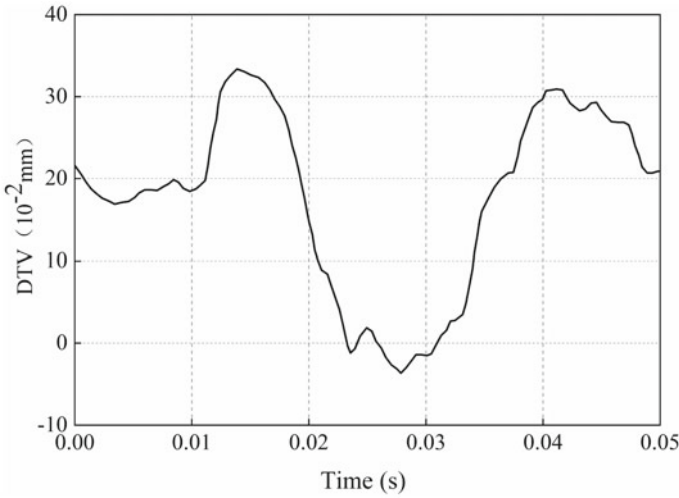


Fig. 3 The initial DTV of brake disc

The initial surface run-out of the brake disc can be measured by the displacement sensor during the uniform rotation of the rotor at the initial braking speed, as shown in Fig. 4.

It can be seen from Figs. 3 and 4 that both DTV and SRO curves have second-order characteristics. The values of DTV and SRO changing with time were converted to those changing with angle, and then the converted DTV and SRO were superimposed,

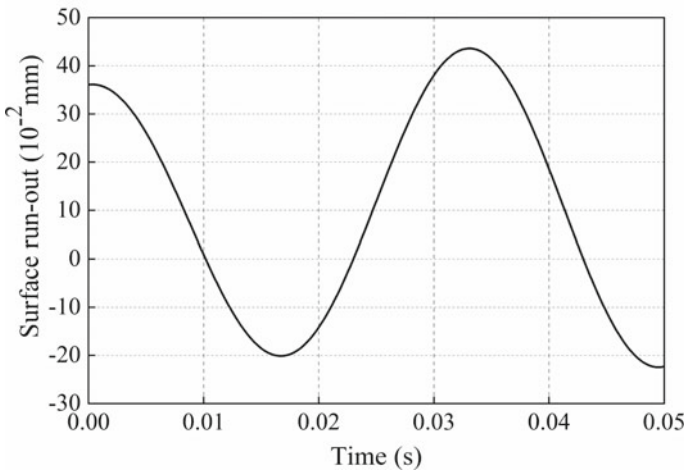


Fig. 4 The initial SRO of brake disc

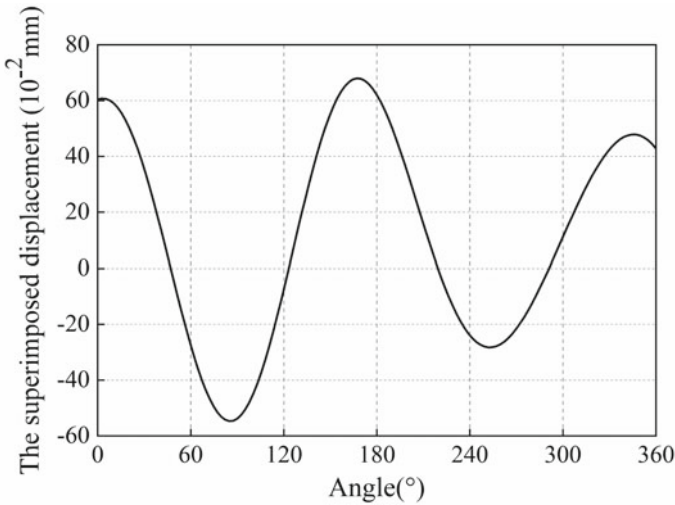


Fig. 5 Displacement curve after superposition of SRO and DTV

and the superimposed displacement curve was shown in Fig. 5. It also has the second-order characteristics and will be used as the system input of the dynamic system simulation.

2.4 Verification of Model

Vehicle brake judder is typically quantified in terms of BPV and BTV [12, 13]. So, in order to verify the correctness of disk-pads spring contact dynamics model in reflecting the phenomenon of brake judder, it is necessary to compare the simulation results of BPV and BTV with the test results.

In order to ensure the comparability between simulation results and test results, the initial conditions of simulation analysis and test should be consistent, including the initial braking pressure, initial braking speed and the input of geometric irregularities in the same brake disc surface. More specific information concerning the bench test of the brake judder can be found in the references [14].

The actual BPV and BTV of the braking system were obtained by bench test. Test process started from the initial braking speed and ended when the speed dropped to 0 km/h. The basic conditions of the test are shown in Table 1.

According to Fig. 1, Matlab/Simulink software was used to develop the Simulink model of the brake. The initial DTV, SRO and system parameters were input into Simulink model, and the BPV and BTV were obtained by simulation. Refer to Appendix A for system parameters of this model. Due to space limitation, the analysis of simulation results and test results of a braking condition (initial brake pressure

Table 1 Basic condition of bench test

Category	Value	Category	Value
Moment of inertia	83.9 kg·m ²	Brake effective radius	132.5 mm
Dynamic radius of tire	358 mm	Deceleration	3.92 km/h
Initial braking speed	120 km/h	Environment temperature	25 °C

is 2.5 MPa) is presented, and similar conclusions can be obtained under other brake pressure conditions.

It can be seen from Figs. 6 and 7 that although the amplitudes and frequencies of the simulation results are inevitably different from the test results to some extent, the overall trend of the simulation results agrees well with the test results. Obviously, the test results are larger than the simulation results, which is preliminarily thought to be due to some unrealistic assumptions in the model development and ignorance of the influence of thermal factor. In the early stage of braking, the reason for the gradual increase of the brake torque variation was mainly that the complete contact between brake block and brake disc requires a certain response time. In the later braking period, thermal expansion and thermal deformation of disc occurred due to friction heat generation, resulting in transient disc thickness variation on the brake disc surface, which aggravated the geometric irregularities of brake disc, and further increased the fluctuation of brake pressure and brake torque.

The maximum BPV of the simulation and dynamo test are 8.8 MPa and 10.4 MPa, and the simulation result is very close to the test data. The maximum BTV of the test is 54.2 N·m. The maximum BTV of the simulation is 38 N·m, which is also close to the test result. Therefore, the BTV and BPV results of the simulation follow the

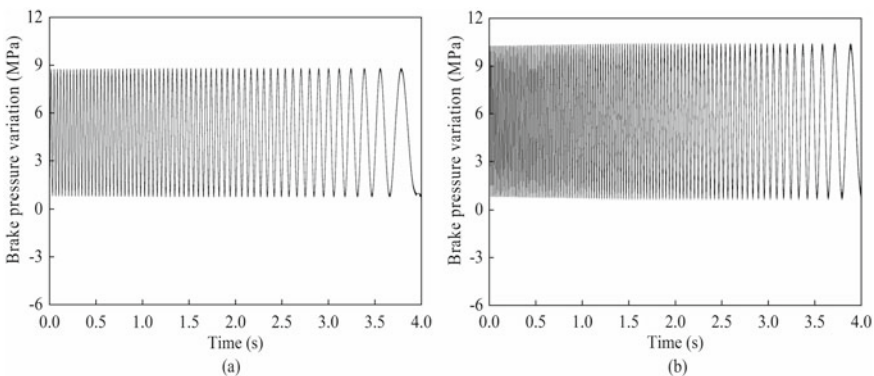


Fig. 6 Time-domain responses of BPV: **a** Simulation result; **b** Bench test result

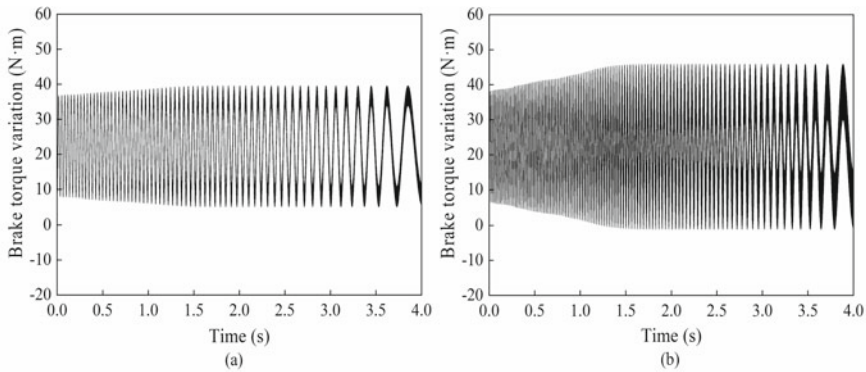


Fig. 7 Time-domain responses of BTV: **a** Simulation result; **b** Bench test result

test data successfully, which indicates that the model is an effective method to study the mechanism of brake judder.

3 Optimization of Brake Judder

3.1 The Key Influencing Parameters of Brake Judder

Because BPV and BTV are the excitation source of brake judder, the method to reduce brake judder is to decrease the magnitude of BPV and BTV. It can be seen from Eqs. (13) and (14) that the main factors affecting BPV and BTV are as follows:

- (1) The geometric irregularities of the inner and outer brake disc surface, that is, DTV and SRO.
- (2) The hydraulic stiffness (K_{hc}) and damping (C_{hc}) of wheel cylinder.
- (3) The dynamic compressive stiffness (K_p) and damping (C_p) of brake block.
- (4) The axial displacement of piston (w_h) and caliper (w_c), and the friction characteristic between brake pad and disc.

At present, there are few studies on reducing brake judder by changing the hydraulic stiffness and damping of wheel cylinder and by changing the dynamic compressive stiffness and damping of brake block. Therefore, this paper carries on the optimization of brake judder from these two aspects.

The evaluation equations of the optimization effect of braking judder are as follows.

$$O_1 = \frac{P_{BTV1\max} - P_{BTV0\max}}{P_{BTV0\max}} \times 100\% \tag{15}$$

$$O_2 = \frac{P_{BPV1\max} - P_{BPV0\max}}{P_{BPV0\max}} \times 100\% \tag{16}$$

where $P_{BTV1\max}$ represents the maximum BTV of improved disc brake; $P_{BTV0\max}$ represents the maximum BTV of original disc brake; $P_{BPV1\max}$ represents the maximum BPV of improved disc brake; $P_{BPV0\max}$ represents the maximum BPV of original disc brake.

Since there is no clear range of the criteria for brake judder optimization, the criterion adopted in this paper is that, when satisfying the requirements of $O_1 \geq 20\%$ and $O_2 \geq 20\%$, the optimization scheme is considered to be effective.

3.2 Improved Design of Caliper Structure

According to Eq. (13), the smaller hydraulic stiffness and damping is, the smaller BPV will be. On the premise of ensuring the safety and reliability of disc brake, in order to reduce the hydraulic stiffness and damping of wheel cylinder, this paper proposes to change the diameter of piston cylinder (the diameter of piston changes accordingly).

According to the improvement scheme shown in Fig. 8, the three-dimensional (3D) model of caliper body was constructed by using CATIA software, as shown in Fig. 9. It can be seen that the difference between original caliper and improved caliper is that the radius of piston cylinder was changed, that is, $r_0 > r_1$ or $r_0 < r_1$.

r_0 is the radius of original piston cylinder with a value of 26 mm. When the inner radius of the piston cylinder meets $r_0 < r_1$, the contact area between brake fluid and piston increases. Therefore, according to Eq. (17), the hydraulic stiffness and

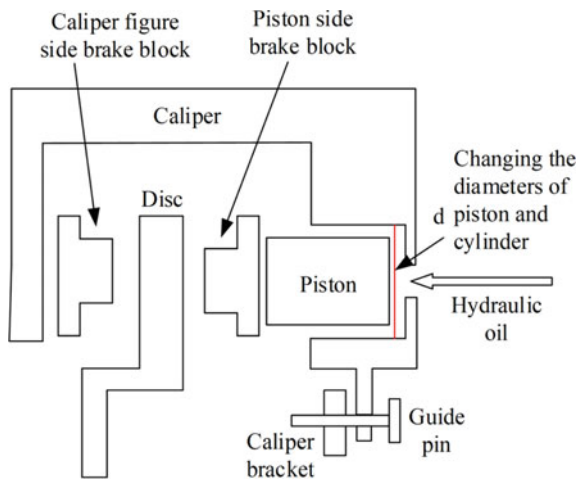


Fig. 8 Schematic diagram of improvement method of caliper structure

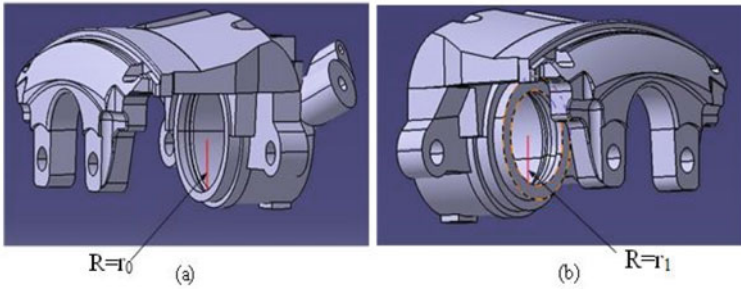


Fig. 9 Three-dimensional model of: **a** original caliper body; **b** improved caliper body

damping of wheel cylinder decreases with the decrease of brake hydraulic pressure under the condition that the same magnitude of braking force is applied. The radius (r_1) of optimized piston cylinder is 30 mm.

$$P = \frac{F}{S} \tag{17}$$

where P is hydraulic pressure, which can be measured by oil pressure sensor; F is the force exerted by piston on brake pad; S is the contact area between piston and brake fluid.

The magnitude of damping is much less than that of hydraulic stiffness, so it can be ignored. The hydraulic stiffness of wheel cylinder can be determined by the following equations.

$$K'_{hc} = \frac{F}{h} \tag{18}$$

In the above, h is the traveling displacement of piston. By substituting Eq. (17) into Eq. (18) can be obtained:

$$K'_{hc} = \frac{P \cdot S}{h} \tag{19}$$

The traveling displacement of piston, the surface area of piston and brake pressure are known quantities. By substituting each parameter value into above equation, the hydraulic stiffness value of optimized caliper body can be obtained. The hydraulic stiffness value after optimization is 6.2×10^5 N/m.

3.3 Improved Design of Brake Pad Backplate

According to Eq. (14), the smaller dynamic compressive stiffness and damping of brake block is, the smaller BTV will be. Since the magnitude of damping is much less than that of compressive stiffness, it can be ignored. Because changing the mass of the object can change the stiffness of the object, this paper, on the premise of ensuring the safety and reliability of the disc brake, proposes to change the compressive stiffness of brake block by slotting brake pad backplate.

As shown in Fig. 10, this paper proposed three design schemes of groove layouts on brake pad backplate. The effective area of brake pad backplate is 4825 mm^2 . The design size of a single transverse groove on backplate surface is $80 \times 4 \text{ mm}$, and the depth of groove is 1 mm. One transverse groove, two transverse grooves and three transverse grooves were designed respectively on the backplate surface, and the percentages of slotted area in total area of the backplate were 6.6% , 13.3% and 19.9% , respectively. Excessively large groove size on the steel back surface will lead to a sharp decrease in the stiffness of brake block and affect the manufacturing process of brake block. Therefore, the percentage of slotted area in total area of the backplate shall not be more than 25% [15]. In order to reduce BTV as much as possible, the mass of backplate should be decreased as much as possible within a reasonable range, so the scheme of making three transverse grooves in the backplate was chosen. The 3D model of improved brake pad backplate is shown in Fig. 11. The mass of improved backplate is reduced by 11.1% compared to the original one, and the compressive stiffness of brake block will also be reduced accordingly.

The dynamic compressive stiffness of brake block can be determined by combining the results of finite element analysis and theoretical calculation. The

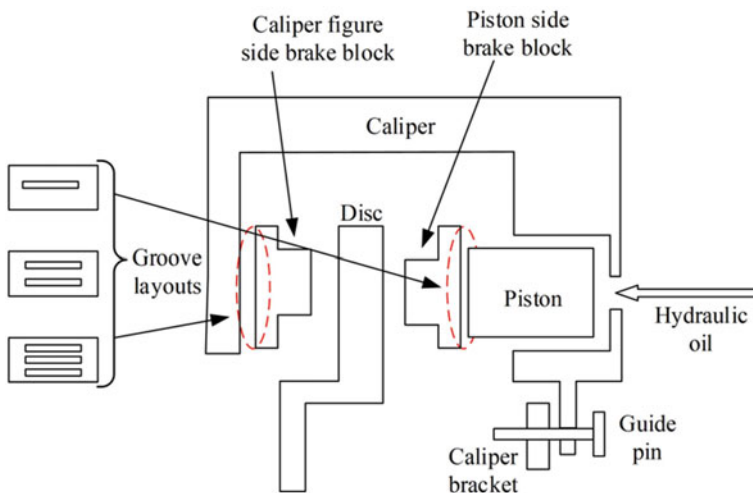


Fig. 10 Schematic diagram of improvement method of brake pad backplate

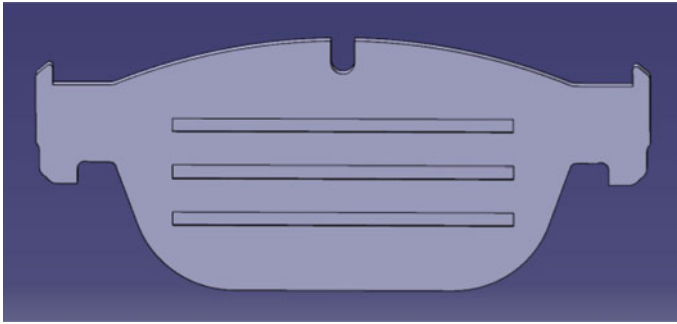


Fig. 11 Schematic diagram of improved brake pad backplate

finite element model of disc brake was established based on a simplified 3D model of an actual disc brake in ANSYS 15.0 software package. In this model, the material properties for each part of disc brake are shown in Table 2.

In the finite element analysis, the mesh type of brake disc and pad is hexahedral mesh, so each grid cell on its surface has 4 nodes, as shown in Fig. 12. It is assumed that the nodes on grid cells of the contact surface between brake disc and pad correspond one to one, and the contact stiffness of each node can be calculated according to Eq. (20).

$$K_{n1} = \frac{f}{h_1} \tag{20}$$

where f is the stress at the node; h_1 is the relative displacement at the node.

Since the four nodes of each grid cell on the contact surface are in parallel with each other, the contact stiffness of each grid cell can be calculated by the following equation.

$$\frac{1}{K_n} = \frac{1}{\sum_{i=1}^4 K_{ni}} \tag{21}$$

Table 2 Material properties for each part of disc brake

Part	Density	Young's modulus/(MPa)	Poisson's ratio
Disc	7000	110,000	0.25
Brake caliper	7000	110,000	0.25
Piston	7200	150,000	0.28
Brake pad backplate	7800	200,000	0.28
Brake pad	2610	9600	0.30

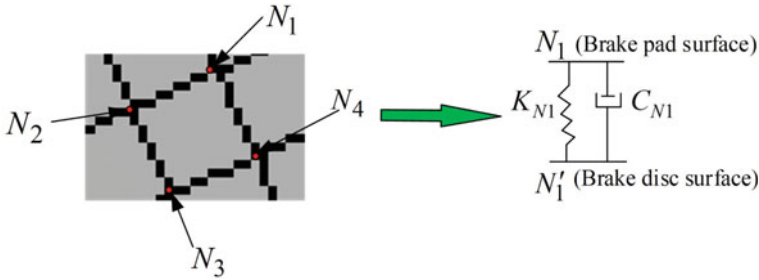


Fig. 12 Diagram of grid nodes between brake disc and pad

According to the surface spring contact dynamic model constructed in this paper, K_{ni} can be assumed to be equal, thus Eq. (21) can be simplified as:

$$K_n = 4K_{ni} \tag{22}$$

According to Eqs. (20) and (22), the calculation equation of contact stiffness between brake disc and pad can be deduced.

$$K'_p = \frac{4N_1 \cdot f}{h_1} \tag{23}$$

where N_1 is the number of grid cells on the contact area between brake disc and pad.

f , h_1 and N_1 were obtained by finite element analysis. According to the above equations, the dynamic compressive stiffness of brake block can be determined. The compressive stiffness value after optimization is 3.42×10^8 N/m, which is 47.4% less than before optimization.

4 Verification of Improved Design

It is known that changing the mass of structure can change the stiffness of structure, so the stiffness values in the whole braking system change correspondingly, and the parameter values can be determined by the same method mentioned above. The parameters of the improved disc brake were all changed within a reasonable range to ensure the stability and safety of braking efficiency.

The system parameters of improved disc brake are shown in Table 3. It can be seen that the contact stiffness and damping of each part of disc brake have been reduced to a certain extent. With the decrease of the hydraulic stiffness and damping of wheel cylinder and the dynamic compressive stiffness and damping of brake block, BPV and BTV will be reduced accordingly. In order to further verify the reliability of the optimization scheme, the simulation and test of brake judder was performed.

Table 3 System parameters of optimized disc brake

Parameter	Value	Parameter	Value	Parameter	Value
m'_c	1.38 kg	K'_{pc}	1.78×10^8 N/m	C'_{ap}	5.7 N · s/m
m'_h	0.10 kg	K'_{ap}	5×10^6 N/m	C'_{ac}	3.56 N · s/m
m'_p	0.40 kg	K'_{ac}	2×10^6 N/m	μ'_h	0.075
R'_{eff}	0.145 m	C'_{hc}	0.18 N · s/m	μ'_p	0.36
K'_{hc}	6.2×10^5 N/m	C'_h	0.29 N · s/m	μ'_{ap}	0.072
K'_h	2.7×10^7 N/m	C'_p	20 N · s/m	μ'_{pc}	0.068
K'_p	3.42×10^8 N/m	C'_{pc}	0.19 N · s/m		

4.1 Simulation Analysis of the Improved Barking System

In order to make the results before and after optimization comparable, it is necessary to ensure that the input conditions and system parameters are consistent. The time-domain responses of BPV and BTV during braking can be obtained by Matlab/Simulink.

Figure 13 shows the BPV simulation result of the improved disc brake. Figure 14 shows the BTV simulation result of the improved disc brake. As can be seen from Figs. 13 and 14, the maximum BPV and BTV of optimized disc brake are significantly reduced compared with those before optimization. For a clearer comparison of optimization effect, the maximum BPV and the maximum BTV are listed in Table 4. The maximum BPV of optimized disc brake was reduced by 30.7% compared with that before optimization, meeting the standard of more than 20%. The maximum BTV of original disc brake and improved disc brake are 38 N · m and 25 N · m, respectively. The maximum BTV of optimized disc brake was 34.2% less than that before optimization, which also satisfied the specified condition. The simulation results show that the improved method proposed in this paper can make the maximum BPV and BTV reach the optimization standard. Thus, the possibility of brake judder occurring can be reduced, which indicates that the optimization methods of brake judder proposed in this paper are reasonable and correct.

5 Conclusion

In this study, the optimization research of a disc brake was carried out based on the established disc-pads surface contact dynamic model of disc brake. The results are as follows.

- (1) The disc-pads spring contact dynamic model proposed in this paper can accurately reflect the characteristics of brake judder, and the simulation results of

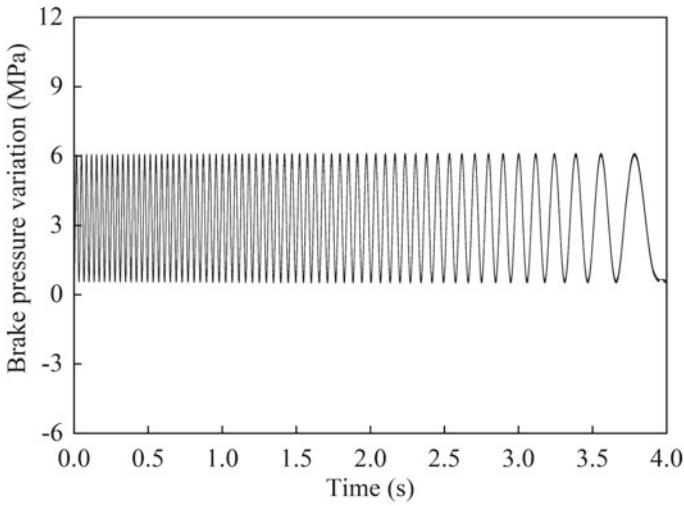


Fig. 13 Simulation result of BPV according to time after optimization

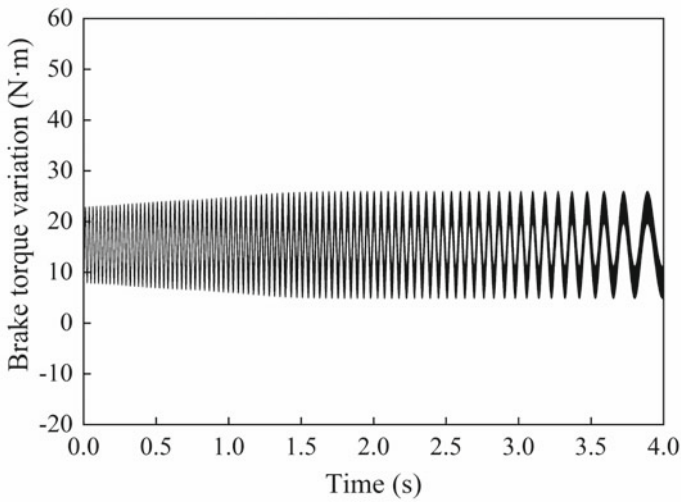


Fig. 14 Simulation result of BTV according to time after optimization

Table 4 Comparison of simulation results before and after optimization

Category	Before optimization	After optimization	Comparison (%)
BPV _{max}	8.8	6.1	-30.7
BTV _{max}	38	25	-34.2

brake pressure and brake torque are consistent with the test results, which indicates that the dynamic model is correct and effective.

- (2) The theoretical derivation and simulation results show that the equivalent hydraulic stiffness of wheel cylinder and compressive stiffness of brake block have a great effect on the brake judder.
- (3) The results show that the optimal scheme to reduce the maximum BTV and BPV by changing the inner diameter of piston cylinder and slotting brake pad backplate are correct and effective.
- (4) The method of finite element analysis combined with theoretical calculation proposed in this paper can successfully determine the parameters of components of the optimized braking system and greatly shorten the research period.

Optimization of brake caliper and brake pad backplate is proposed to reduce brake pressure and brake torque variation in this paper, which finally successfully reduces the incidence of brake judder. By building a dynamic model of braking system, braking judder can be quantified in the form of braking pressure variation and braking torque variation, which can provide some references for reducing braking judder.

Acknowledgements This work was supported by Jiangsu Hengli Brake Manufacturing Company on the projects “Study on Key Technology of NVH Characteristics of Braking system” (No. 201908), “High Level Innovation and Entrepreneurship Talent” (No. 2019015) of Jingjiang City and Jiangxi Province Key Laboratory of Vehicle Noise and Vibration (No. JXNVHKB-KFKT-201802).

Appendix A

Table A.1 The parameter values involved in the simulation process

Category	Symbol	Value	Category	Symbol	Value
Mass of caliper	m_c	1.5 kg	Stiffness of sliding joint between caliper and bracket	K_{ac}	3.3×10^8 N/m
Mass of piston	m_h	0.12 kg	Stiffness of abutment shim between pad and caliper bracket	K_{ap}	4×10^5 N/m
Mass of brake block	$m_{p1} = m_{p2}$	0.45 kg	Contact stiffness between brake block and caliper	K_{pc}	2×10^8 N/m

(continued)

(continued)

Category	Symbol	Value	Category	Symbol	Value
Inner radius of brake disc	r_1	0.085 m	Equivalent hydraulic stiffness	K_{hc}	$7.8 \times 10^6 \text{ N/m}$
Effective friction radius	R_{eff}	0.133 m	Interface stiffness between inner brake block and piston	K_h	$3.5 \times 10^8 \text{ N/m}$
Thickness of disc	H_d	0.024 m	Compressive stiffness of brake block	K_p	$6.5 \times 10^8 \text{ N/m}$
Outer radius of brake disc	r_2	0.17 m	The rotational stiffness of brake blocks around the fixed points	$K_{11} = K_{12}$	$1.53 \times 10^4 \text{ N} \cdot \text{m/rad}$
Density of disc	ρ	$7.80 \times 10^3 \text{ kg/m}^3$	Damping of abutment shim between pad and caliper bracket	C_{ap}	$6.0 \text{ N} \cdot \text{s/m}$
Poisson's ratio	ν	0.3	Damping of sliding joint between caliper and bracket	C_{ac}	$4.0 \text{ N} \cdot \text{s/m}$
Equivalent hydraulic damping of wheel cylinder	C_{hc}	$0.2 \text{ N} \cdot \text{s/m}$	Damping between piston and brake block	C_h	$0.3 \text{ N} \cdot \text{s/m}$
Inertia moment of brake blocks	$I_{p1} = I_{p2}$	$2.26 \times 10^{-4} \text{ kg} \cdot \text{m}^2$	Compressive damping of brake block	C_p	$22 \text{ N} \cdot \text{s/m}$
Surface area of piston	S	28.27 cm^2	Damping between brake block and caliper	C_{pc}	$0.2 \text{ N} \cdot \text{s/m}$
Coefficient of friction between pads and rotor	μ_p	0.4	Coefficient of friction between piston and brake block	μ_h	0.09

(continued)

(continued)

Category	Symbol	Value	Category	Symbol	Value
Distance between the center of mass of the brake block and its connection point with the caliper bracket	$L_{21} = L_{22}$	0.06 m	Coefficient of friction between caliper bracket and brake block	μ_{ap}	0.08
Coefficient of friction between brake block and caliper	μ_{pc}	0.08			

References

- Kim J, Lee M, Kim B, Cho C (2013) A prediction of the relation between the disc brake temperature and the hot judder critical speed. *Trans Korean Soc Automot Eng* 21(1):61–67
- de Vries A, Wagner M (1992) The brake judder phenomenon. SAE Technical Paper
- Lee CF, Savitski D, Manzie C, Ivanov V (2015) Active brake judder compensation using an electro-hydraulic brake system. *SAE Int J Commer* 8(1)
- Jacobsson H (2003) Aspects of disc brake judder. *Proc Inst Mech Eng, Part D: J Automob Eng* 217
- Sim KS, Lee JH, Park TW, Cho MH (2013) Vibration path analysis and optimal design of the caliper for brake judder reduction. *Int J Automot Technol* 14(4):587–594
- Bryant D, Fieldhouse JD, Talbot CJ (2011) Brake judder-an investigation of the thermo-elastic and thermo-plastic effects during braking. *Int J Vehicle Struct Syst* 3(1):58–73
- Jung SP, Kim YG, Park TW (2012) A study on thermal characteristic analysis and shape optimization of a ventilated disc. *Int J Precis Eng Manuf* 13(1):57–63
- Leslie AC (2004) Mathematical model of brake caliper to determine brake torque variation associated with disc thickness variation (DTV) input. SAE Technical Paper
- Zhang L, Quan X (2009) Brake judder analysis based on single-point contact model. In: *Proceedings of the 2009 annual meeting of China society of automotive engineering*
- Jacobsson H (2003) Disc brake judder considering instantaneous disc thickness and spatial friction variation. *Proc Inst Mech Engs, Part D: J Automob Eng* 217(5):325–342
- Sen OT, Dreyer JT, Singh R (2013) Low frequency dynamics of a translating friction element in the presence of frictional guides, as motivated by a brake vibration problem. *J Sound Vib* 332:5766–5788
- Sen OT, Dreyer JT, Singh R (2012) Order domain analysis of speed-dependent friction-induced torque in a brake experiment. *J Sound Vib* 331:5040–5053
- Sen OT, Dreyer JT, Singh R (2013) Envelope and order domain analyses of a nonlinear torsional system decelerating under multiple order frictional torque. *Mech Syst Signal Process* 35:324–344

14. Pan G, Liu P, Xu Q, Chen L (2020) Brake judder analysis based on dynamic model of disc-pad spring contact. *J Chongqing Univ Technol (Natural Science)*
15. Massi F, Berthier Y, Baillet L (2008) Contact surface topography and system dynamics of brake squeal. *Wear* 265(11):1784–1792